THERMOCHEMICAL BREAKDOWN OF A GRAPHITE BODY IN A HYPERSONIC GAS STREAM

V. N. Bertsun, A. M. Grishin, and N. G. Ismailov

UDC 533.6.01 + 536.24

Thermochemical breakdown of bodies in a hypersonic gas stream was investigated in [1-7]. In [2] the phenomenon was first observed of corner points on the profile of a body in a stream. Subsequently, the dynamics of the formation and movement of corner points was analyzed qualitatively and quantitatively in [3-5] without allowing for heat transfer in the body. The mass ablation on a three-dimensional body on a given flight trajectory was investigated in [6], and in [7] the area rule was proposed for determining the heat-transfer coefficient.

The present paper proposes a simple method for determining the mass ablation rate for graphite materials, without using the concept of effective enthalpy. In this method one can allow for the transient nature of the process and the redistribution of heat in the solid, and also determine the mass ablation rate from sublimation and heterogeneous chemical reactions.

An algorithm is proposed for numerical solution of two-dimensional unsteady thermochemical breakdown, and results are given for fixed and variable incident flow parameters. It is shown that in turbulent flow the shape of the body resulting from thermochemical breakdown differs qualitatively from that in laminar flow. The influence of anisotropy on the temperature field in the body is investigated. It is established that the corner points on the wetted surface [4] do not disappear when flow of heat in the body is allowed for. It is shown that the "external" and "internal" features of the unsteady process [8-10] interact along the flight trajectory.

1. We consider thermochemical breakdown of a graphite body having the initial shape of a spherically blunted cone (Fig. 1, which also shows the coordinate system used) in a hypersonic gas stream under the following basic assumptions:

1. The Reynolds number in the incident stream $\mathrm{Re}_\infty \gg 1$, and a frozen boundary layer is formed near the body surface.

At the outer edge of the boundary layer the air is in a state of thermodynamic equilibrium, and is a four-component mixture of O, O_2, N, N_2.

3. The internal surface BCD is either isothermal or adiabatic, and there is neglibly small heat flow in the section AB (see Fig. 1).

4. We shall consider that the following heterogeneous processes take place on the outer body surface*:

$$1)\ C + O_2 \to CO_2; \quad 2)\ 2C + O_2 \to 2CO;$$

$$3)\ C + O \to CO; \quad 4)\ C + CO_2 \to 2CO;$$

$$5)\ C \rightleftarrows C\ (\mathrm{Gas}); \quad 6)\ O + O + C \to O_2 + C;$$

$$7)\ N + N + C \to N_2 + C.$$

Taking account of the above assumptions, we now consider the following boundary problem. Within the solid we have the heat-conduction equation

$$c_s(T)\rho_s \frac{\partial T}{\partial t} = \frac{1}{rL}\left[\frac{\partial}{\partial x}\left(\frac{\lambda_x(T) r}{L}\frac{\partial T}{\partial x}\right) + \frac{\partial}{\partial y}\left(\lambda_y(T) rL \frac{\partial T}{\partial y}\right)\right],\ 0 < x < x_B, 0 < y < l(x,t), r = r(x,\ y), \qquad (1.1)$$

*The heterogeneous formation reactions for cyanogen CN which occur at very high temperatures are not accounted for in the calculations because the literature does not have reliable data on the kinetics of these reactions. Up to surface temperatures of $T_w \sim 3000°K$ the formation of CN does not influence the mass ablation rate.

Tomsk. Translated from Zhurnal Prikladnoi Mekhaniki i Tekhnichesloi Fiziki, No. 2, pp. 58-66, March-April, 1982. Original article submitted February 19, 1981.

0021-8944/82/2302-0211$07.50

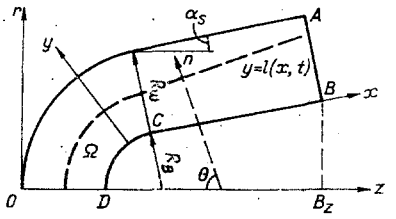

Fig. 1

which must be solved with the initial and boundary conditions

$$T|_{t=0} = T_{\text{н}},\ T|_{y=0} = T_{\text{н}},\ \left(\text{or}\ \left.\frac{\partial T}{\partial y}\right|_{y=0} = 0\right),\ \left.\frac{\partial T}{\partial x}\right|_{x=0} = 0,\ \left.\frac{\partial T}{\partial x}\right|_{x=x_{\text{в}}} = 0; \tag{1.2}$$

$$\lambda_y(T_w)\left.\frac{\partial T}{\partial n}\right|_{y=l(x,t)} = q_w - (\rho v)_w h_w + (\rho v)_w h_{sw} - \varepsilon_s \sigma T_w^4. \tag{1.3}$$

The equation to determine the ambient body surface shape has the form

$$\frac{\partial l}{\partial t} = -V_n(x,t)\sqrt{1+\left(\frac{1}{1+l\varkappa}\frac{\partial l}{\partial x}\right)^2}, \tag{1.4}$$

for which the initial conditions are

$$l(x,0) = l_0 = R_w - R_{\text{в}},\ l(0,t) = l_0 - \int_0^t V_n(0,t)\,dt, \tag{1.5}$$

where $l(x, t)$ is a function governing the ambient shape of the exterior body surface; and $V_n = (\rho v)_w/\rho_s$ is the linear rate of thermochemical breakdown normal to the exterior body surface.

To determine the concentrations of components of the gas at the body surface c_{iw} ($i = 1,\ldots, 7$) we have the mass balance condition at the surface

$$J_i + (\rho v)_w c_{iw} = R_i,\ J_i = \beta_{iw}(c_{iw} - c_{ie}),\ i = \overline{1,7}, \tag{1.6}$$

where the mass-transfer coefficients β_{iw} are determined with the help of the analog between heat- and mass-transfer processes [11].

Here the following notation is used: r and z, radial and logitudinal cylindrical coordinates; y, distance from an arbitrary point to the basic curve BCD along the normal; x, arc length of the basic curve BCD from the point D to the point of intersection of the curve and the above normal; $L = 1 + y\varkappa(x)$; $\varkappa(x)$, curvature of the basic curve BCD at the point x; x_{B}, arc length BCD; B_z, body length; R_w, and R_{B}, radii of spherical blunting of the exterior and interior surfaces, respectively; α_s, cone semiangle; λ_x, λ_y, c_s, ρ_s, thermal conductivity in the directions along x and y, respectively, the specific heat and the density of the graphite; n, exterior normal to the body surface; T, absolute temperature; t, time; q_w, convective heat flux from the gas; c_i, R_i, h_i, mass concentration, the mass rate of formation and the enthalpy of the i-th component, where the component ordinal number corresponds to the following order — O, O_2, N and N_2, C (gas), CO, CO_2; $h_w = \sum_{i=1}^{7} c_{iw}h_{iw}$, gas enthalpy at the body surface; $(\rho v)_w = \sum_{i=1}^{7} R_i$ mass ablation of material from unit body surface per unit time; h_s, enthalpy of the body material; σ, Stefan–Boltzmann constant; and ε_s, body emissivity. The subscripts e, w and s refer to parameters at the outer edge of the boundary layer, at the outer body surface, and inside the solid, respectively.

2. The molar volume rates of reactions 1-7 have the form [8]

$$U_1 = k_1 \frac{c_{2w}\rho_w}{M_2} \exp\left(-\frac{E_1}{RT_w}\right), \quad U_2 = k_2 \frac{c_{2w}\rho_w}{M_2} \exp\left(-\frac{E_2}{RT_w}\right); \tag{2.1}$$

$$U_3 = k_3 \frac{c_{1w}\rho_w}{M_1} \exp\left(-\frac{E_3}{RT_w}\right), \quad U_4 = k_4 \frac{c_{7w}\rho_w}{M_7} \exp\left(-\frac{E_4}{RT_w}\right); \tag{2.2}$$

$$U_5 = \frac{A_C\left(p_C^* - p_C\right)}{\sqrt{2\pi R M_5 T_w}} \quad U_6 = k_6 \frac{c_{1w}\rho_w}{M_1}, \quad U_7 = k_7 \frac{c_{3w}\rho_w}{M_3}, \tag{2.3}$$

where E_j, k_j are the activation energy and the preexponential factor for the j-th reaction; A_C, accommodation coefficients for graphite ($0 \leqslant A_C \leqslant 1$); p_C^*, pressure of saturated C vapor; p_C, partial pressure of C vapors:

$$p_C = p_e c_{5w} \frac{M_w}{M}, \quad M_w = 1 \Big/ \sum_{i=1}^{7} \frac{c_{iw}}{M_i}, \quad \rho_w = \frac{p_e M_w}{RT_w},$$

M_i is the molecular weight of the i-th component; and R is the universal gas constant.

Using Eqs. (2.1)-(2.3) we obtain the mass rates of formation (or disappearance) of components due to the heterogeneous reactions R_i ($i = 1, \ldots, 7$) and an expression for the mass ablation

$$(\rho v)_w = \sum_{i=1}^{7} R_i = \rho_w \left[\left(\frac{M_2}{M_2} - 1\right) c_{2w}\varphi_1 + \left(\frac{M_6}{M_1} - 1\right) c_{2w}\varphi_2 \right. \tag{2.4}$$

$$\left. + \left(\frac{M_6}{M_1} - 1\right) c_{1w}\varphi_3 + \left(\frac{2M_6}{M_7} - 1\right) c_{7w}\varphi_4 \right] + \frac{M_5 A_C\left(p_C^* - p_C\right)}{\sqrt{2\pi R M_5 T_w}},$$

where $\varphi_j = k_j \exp\left(-E_j/RT_w\right)$ is the rate constant for the j-th reaction.

Table 1 shows the thermokinetic constants used for reactions 1-7 in the calculations. It should be noted that in some references (see, e.g., [14]) data are given for the probability ε_j of the reactions. The probability of the j-th heterogeneous reaction ε_j is linked to the rate constant of the reaction by the relation

$$\varphi_j = \varepsilon_j \sqrt{RT_w}/2\pi M_r, \tag{2.5}$$

where M_g is the molecular weight of the appropriate gas reagent of the j-th reaction.

For the saturation pressure of C vapor we used the temperature dependence

$$p_C^* = \exp\left(30.223 - \frac{85656}{T}\right) \text{ N/m}^2 \tag{2.6}$$

obtained by approximating to the tabular data of [16], where the error in the approximation does not exceed 1%. The enthalpy of the individual components was calculated from the approximation formulas from [17]. The thermophysical characteristics of the various graphite materials used in the calculations were given in [18, 19], and the thermal conductivity as a function of temperature is given by a piecewise-linear approximation to the tabular data, which ensures an accuracy sufficient for practical purposes.

3. The incident stream parameters in the unperturbed zone are determined from the standard earth atmosphere formulas [20] in terms of the geometric height H_∞ from the earth's surface.

TABLE 1

j	k_j, m/sec E_j, cal/mole A_C, ε_j	Source
1	$k_1=15\cdot10^6$, $E_1=58{,}000$	[12]
2	$k_2=8\cdot10^6$, $E_2=37{,}800$	[13]
3	$\varepsilon_3=0.63\exp(-1160/T_w)$	[14]
4	$k_4=16\cdot10^6$, $E_4=85{,}000$	[15]
5	$A_C=0.3$	[29]
6	$\varepsilon_6=\varepsilon_3=0.63\exp(-1160/T_w)$	[14]
7	$\varepsilon_7=0.01$	[21]

The system of equations for calculating the parameters of the gas directly behind the shock wave and at the stagnation point, assuming a binary air model and no ionization has the form [21]

$$\frac{p_1}{p_\infty}=\frac{2\gamma_\infty M_\infty^2}{\gamma_{ef}+1},\quad \frac{T_1}{T_\infty}=\frac{p_1}{p_\infty}\frac{\rho_\infty}{\rho_1}\frac{1}{1+\alpha}; \tag{3.1}$$

$$\frac{\rho_1}{\rho_\infty}=\frac{\gamma_{ef}+1}{\gamma_{ef}-1},\quad \frac{4\alpha^2}{1-\alpha}=\frac{K_C(T_1)}{p_1}; \tag{3.2}$$

$$\frac{\gamma_{ef}-1}{\gamma_{ef}}=f_1(h_0)+f_2(h_0)\lg p_0,\quad h_0=h_\infty+\frac{V_\infty^2}{2}; \tag{3.3}$$

$$\frac{T_0}{T_1}=1+\frac{\gamma_{ef}-1}{2}M_1^2,\quad M_1^2=\frac{\gamma_{ef}-1}{2\gamma_{ef}}; \tag{3.4}$$

$$\frac{p_0}{p_1}=\left(\frac{T_0}{T_1}\right)^{\frac{\gamma_{ef}}{\gamma_{ef}-1}},\quad \rho_0=\frac{\gamma_{ef}}{\gamma_{ef}-1}\frac{p_0}{h_0}, \tag{3.5}$$

where K_C is the equilibrium constant for the binary air model [22]; and f_1 and f_2 are approximation functions for the equation of state for air [23].

System (3.1)-(3.5) is solved with the aid of an iteration process in γ_{ef}, the initial approximation taken is γ_{ef} = 1.25 ($1 \leqslant \gamma_{ef} \leqslant 1{,}4$) the functions f_1 and f_2 are given tabularly, and quadratic interpolation is performed when necessary.

In Eqs. (3.1)-(3.5) and below p is the pressure, V is the velocity, ρ is the density, h is the enthalpy, γ is the adiabatic index, M is the Mach number, α is the degree of dissociation for the binary air model, and the subscripts ∞, 1 and 0 refer to parameters in the unperturbed flow, immediately behind the normal shock wave, and at the stagnation point, respectively, while the subscript ef corresponds to effective values.

The pressure at the outer edge of the boundary layer is calculated from the modified Newtonian formula [22]

$$p_e/p_0=\cos^2\theta+(p_\infty/p_0)\sin^2\theta, \tag{3.6}$$

where θ is the angle between the normal n and the direction opposite to the z axis (see Fig. 1).

The parameters V_e, ρ_e, T_e are calculated with the aid of formulas for isentropic flow of a gas with the effective adiabatic index γ_{ef}:

$$\frac{V_e^2}{2h_0}=1-\left(\frac{p_e}{p_0}\right)^{\frac{\gamma_{ef}-1}{\gamma_{ef}}},\quad \frac{\rho_e}{\rho_0}=\left(\frac{p_e}{p_0}\right)^{\frac{1}{\gamma_{ef}}},\quad \frac{T_e}{T_0}=\left(\frac{p_e}{p_0}\right)^{\frac{\gamma_{ef}-1}{\gamma_{ef}}}. \tag{3.7}$$

It should be noted that the postulate of isentropic gas flow at the outer edge of the boundary layer is valid even for $\mathrm{Re}_\infty=\frac{\rho_\infty V_\infty}{\mu_\infty}R_w \gtrsim 10^4$ [23], since in this case we can neglect the variation in entropy along the outer edge of the boundary layer.

The dynamic viscosity μ_e is calculated from the Sutherland formula with a correction for dissociation [22]. The concentrations c_{ie} (i = 1,..., 4) are determined from the equilibrium equations [22]:

$$\frac{c_{1e}^2}{c_{2e}}=\frac{150000}{\rho_e}\exp\left(-\frac{59500}{T_e}\right),\quad c_{1e}+c_{2e}=0.235; \tag{3.8}$$

$$\frac{c_{3e}^2}{c_{4e}}=\frac{130000}{\rho_e}\exp\left(-\frac{113000}{T_e}\right),\quad c_{3e}+c_{4e}=0.765. \tag{3.9}$$

The enthalpy h_e is determined from the Bernoulli relation.

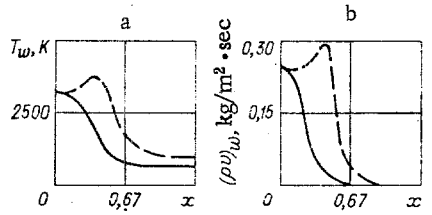

Fig. 2

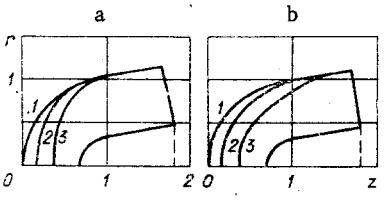

Fig. 3

To calculate the convective heat flux from the gas q_w we have many different approximate formulas [22], obtained by analytical methods or resulting from numerical computations and the data of experimental investigations. There are estimates that all these formulas have the same accuracy. Therefore, here we use formulas which are the simplest to mechanize on a computer.

The heat flux at the forward stagnation point is calculated from the Fenster formula for frozen flow in the boundary layer [24]

$$q_{w0} = 0.09 V_\infty^{1.96} \sqrt{R_w \frac{p_M}{p_0}}, \tag{3.10}$$

where p_m is the sea level pressure, and quantities are in SI units.

To determine the heat flux over the body surface we use formulas from [1]: for laminar flow conditions

$$q_w = q_{w0}(0.55 + 0.45 \cos 2\theta); \tag{3.11}$$

for turbulent

$$q_w = q_{wT}\,(2.5 \sin\theta - 2.3 \sin^3\theta), \tag{3.12}$$

where q_{wt} is the maximum heat flux in the turbulent region near the sonic line. According to [22],

$$q_{wT} = q_{w0} 10.637 (R_w \rho_\infty)^{0.3}. \tag{3.13}$$

We allowed for the influence of blowing of ablation products and the nonisothermal condition of the wetted surface on the heat- and mass-transfer characteristics by the approximate method of [25].

4. For convenience of calculating the temperature field in the solid we carried out the coordinate transformation $\bar{y} = y/l(x, t)$, which converts the time-variant region Ω (see Fig. 1) into a rectangle. An algorithm for numerical solution of the above problem consists of three basic steps: 1) at $t = t_n$ ($n = 0, 1, 2, \ldots$) from the known temperature and body surface shape we calculate all the parameters governing the right side of the heat balance equation on the body surface, Eq. (1.3); 2) by solving the heat-conduction equation (1.1) with boundary conditions (1.2) and (1.3) we determine the temperature field in the solid; 3) with the new surface temperature we determine the mass ablation rate $(\rho v)_w$, and by solving Eq. (1.4) we determine the new surface position for $t = t_{n+1} = t_n + \tau$, where τ is the time step.

For numerical solution of the heat-conduction equation (1.1) with the appropriate boundary conditions we use the split-direction method [26], and to solve locally one-dimensional problems we use a two-layer implicit difference scheme obtained on the basis of an iteration–interpolation method [27].

To solve the equation for displacement of the surface, Eq. (1.4), for the derivative with respect to the space variable, we use a left-difference approximation, since according to [5], the use of central differences can lead to instability in the calculation.

Comparison of the values for the mass ablation rate $(\rho v)_w = 0.17; 0.24; 0.30$ kg/m²·sec obtained near the forward stagnation point with $p_0 = 10^5$ N/m², $R_w = 0.015$ m for $T_w = 3000; 3500; 3700$°K, respectively, using the above method, with the experimental data presented in [28], where for $p_0 = 10^5$ N/m², $R_w = 0.018$ m the corresponding values are $(\rho v)_w = 0.16; 0.22; 0.32$ allows us to establish that with this method one can obtain the characteristics of thermochemical breakdown with an accuracy that is acceptable in practice.

5. From results of calculations of model heat problems without accounting for breakdown of the body we studied the influence of the degree of anisotropy of the thermal proper-

TABLE 2

t, sec	0	10	20	30	40
H_∞, m	65,000	57,000	48.000	38,000	25,000
V_∞, m/sec	7,700	7,600	7,500	6.000	5.000

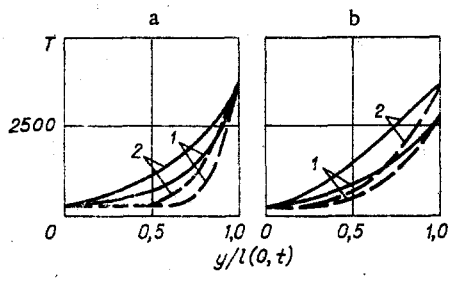

Fig. 4

ties of various graphite materials in a temperature field. It was observed that the flow of heat over the body in the case of an isothermal BCD surface affects the temperature field appreciably only in the case $(\lambda_x/\lambda_y) \gg 1$, i.e., when the thermal conductivity along the body considerably exceeds the thermal conductivity along the normal to the base curve (in direction y). Thus, for $(\lambda_x/\lambda_y) \leqslant 1$, which is typical for most graphite materials used in aviation and space and rocket engineering, one can calculate the temperature field in a solid, if the BCD surface is isothermal, in a locally one-dimensional formulation with respect to y. This possibility was implemented in subsequent calculations whose results are presented below.

By way of example, Figs. 2 and 3 show results of calculations using the above scheme for thermochemical breakdown of an initially spherically blunted cone of semivertex angle 10°, made of grade VPP graphite [18] for fixed incident flow incident flow parameters: H_∞ = 40,000 m, V_∞ = 7500 m/sec.

Figure 2a, b shows the distributions of surface temperature T_w and local mass ablation rate $(\rho v)_w$, typical for a laminar flow case (solid lines) and with a zone of transition from laminar to turbulent flow (broken lines). Figure 3a, b respectively, show the body surface shapes resulting from breakdown in laminar flow and in flow with a transition zone, for various values of time. The linear dimensions in Figs. 2-4 are referenced to the radius of blunting of the initial shape, and the time $\bar{t}$ in Fig. 3 is dimensionless (curve 1 corresponds to $\bar{t} = 0$, curve 2 to $\bar{t} = 1$, and curve 3 to $\bar{t} = 2$). It can be seen from analysis of Figs. 2-4 that the presence of a transition zone promotes more intense breakdown of the front part of the body, compared with breakdown in laminar flow. This is associated with the occurrence of a maximum of temperature and of mass ablation rate in the region of transition from laminar to turbulent flow.

It is curious that in calculations of the free surface using the technique discussed we locate protuberances which can be interpreted as corner points, observed in [2]. The basic rules for the behavior of corner points are those given in [2-4]. In particular, breakdown conditions are obtained where one sees several corner points and their migration.

It is of interest to analyze the temperature field in the solid. Figure 4 shows the temperature profiles on the body axis OD (see Fig. 1) at different times, as obtained by the technique suggested (solid curves), and the corresponding quasi-stationary temperature profiles (broken curves), obtained analytically:

$$y = \int_T^{T_w} \frac{\lambda_y(T)\,dT}{(\rho v)_w \int_T^{T_w} c_s(T)\,dT - q_s} + l(0, t). \qquad (5.1)$$

In deriving this formula we assumed that the internal boundary layer of the graphite heat shield material is isothermal, and that on the surface there is a given flux to the wall q_s. In the calculations using Eq. (5.1), whose results are shown in Fig. 4, the values of q_s and T_w were taken from calculations using the suggested technique. It is evident that in this case there will be a minimum difference between the temperature fields obtained from Eq. (5.1) and from solution of the problem of Eqs. (1.1)-(1.6).

Figure 4a shows the results of calculations for fixed conditions of the incident flow (the curves 1 correspond to t = 2, 2 to t = 5 sec), and Fig. 4b shows the results of calculations along the trajectory [30] given in Table 2 (the curves 1 correspond to t = 10, curve 2 to t = 30 sec). The solid curves correspond to calculations using the method described in the reference, and the broken lines correspond to calculation using Eq. (5.1).

It follows from analysis of Fig. 4a and b that the quasistationary temperature curves differ appreciably from the exact values obtained by numerical integration of the unsteady equations. It is curious that for the flight along the given trajectory the level of difference increases with increasing time. In other words, the change in conditions at the outer edge of the boundary layer ("external unsteadiness" in the terminology of [8, 10]) leads to a change in the temperature field inside the heat shield material (HSM), i.e., produces the so-called "interior unsteadiness [8, 10]. This effect stems from the fact that the characteristic time for change in the parameters of state at the outer edge of the boundary layer coincides in order of magnitude with the thermal relaxation time in the solid $t_{se} \sim 0.05R_w^2/a_s$, where a_s is the characteristic diffusivity. In this case the movement of corner points at the interface of the media leads to an additional unsteadiness of the process in the solid.

It should be noted that the temperature field in the HSM layer has a very great influence on the stress field, while the latter has a strong influence on mechanical ablation of the HSM.

Thus, this example confirms the concept of [8, 10] of interaction of the "exterior" and "interior" unsteadinesses as vehicles traverse their trajectories.

LITERATURE CITED

1. I. N. Murzinov, "The shape of bodies ablating under intense heating during motion in the atmosphere," Izv. Akad. Nauk SSSR, Mekh., No. 4 (1965).
2. V. G. Konyaev, "Analytical investigation of the change in shape of ablating bodies moving at supersonic speed in the atmosphere," Uch. Zap. TsAGI, 5, No. 6 (1974).
3. V. V. Lunev, "Some properties and solutions of the ablation equation," Izv. Akad. Nauk SSSR, Mekh. Zhidk. Gaza, No. 3 (1977).
4. V. G. Voronkin, V. V. Lunev, and A. N. Nikulin, "The stationary shape of bodies ablating due to aerodynamic heating," Akad. Nauk SSSR, Mekh. Zhidk. Gaza, No. 2 (1978).
5. V. V. Znamenskii, "Numerical solution of the ablation equation," Izv. Akad. Nauk SSSR, Mekh. Zhidk. Gaza, No. 2 (1978).
6. É. Z. Apshtein, N. N. Pilyugin, and G. A. Tirskii, "Mass ablation and change of shape of a three-dimensional body in motion in an earth atmospheric trajectory," Kosm. Issled., 17, 2 (1979).
7. É. Z. Apshtein and N. N. Pilyugin, "The rule of areas for the heat-transfer coefficient for three-dimensional ablating bodies with heat fluxes dependent on the local surface slope," Izv. Akad. Nauk SSSR, Mekh. Zhidk. Gaza, No. 2 (1979).
8. A. M. Grishin, Mathematical Modeling of Some Unsteady Aerothermochemical Phenomena [in Russian], Tomsk State Univ. (1973).
9. A. M. Grishin and V. I. Zinchenko, "Coupled heat and mass transfer between a reactive solid and a gas in the presence of nonequilibrium chemical reactions," Izv. Akad. Nauk SSSR, Mekh. Zhidk. Gaza, No. 2 (1974).
10. A. M. Grishin, "Mathematical modeling of coupled problems in mechanics of reacting media," in: Numerical Methods of Solving Transfer Problems, Part 2 [in Russian], Izd. ITMO im. A. V. Lykov, Akad. Nauk BSSR, Minsk (1979).
11. G. A. Tirskii, "Determination of heat flux near a stagnation point with two-value curvature in flow of a dissociating gas of arbitrary chemical composition over a body," Zh. Prikl. Mekh. Tekh. Fiz., No. 1 (1965).
12. N. V. Lavrov, Physical and Chemical Principles of the Fuel Combustion Process [in Russian], Nauka, Moscow (1971).
13. A. B. Reznikov, I. P. Basina, et al., Combustion of Natural Solid Fuel [in Russian], Nauka, Alma-Ata (1968).

14. Park, "Influence of atomic oxygen on ablation of graphite," Raketn. Tekh. Kosmon., 14, 11 (1976).
15. G. P. Khaustovich, "Interaction of carbon and carbon dioxide in the range 1300-3100°K," Zh. Fiz. Khim., 42, 7 (1968).
16. L. V. Gurvich, G. A. Khachkuruzov, et al., Thermodynamic Properties of Specific Substances [in Russian], Vol. 2, Akad. Nauk SSSR, Moscow (1962).
17. L. V. Gurvich and N. P. Rtishcheva, "Analytical representation of tabular values of the thermodynamic properties of gases," Teplofiz. Vys. Temp., 3, 1 (1965).
18. V. P. Sosedov, Properties of Structural Material Based on Carbon (Handbook) [in Russian], Metallurgiya, Moscow (1975).
19. L. M. Buchnev, V. I. Volga, et al., "Investigation of the enthalpy of carbons in the range 500-3250°K," Teplofiz. Vys. Temp., 11, 6 (1973).
20. Parameters of the Standard Atmosphere, GOST 4401-73 [in Russian], Moscow (1977).
21. V. P. Agafonov, V. K. Vertushkin, et al., Nonequilibrium Physical and Chemical Processes in Aerodynamics [in Russian], Mashinostroenie, Moscow (1972).
22. N. F. Krasnov, Aerodynamics [in Russian], Vysshaya Shkola, Moscow (1971).
23. I. N. Murzinov, "The laminar boundary layer in hypersonic flow of equilibrium dissociating air," Izv. Akad. Nauk SSSR, Mekh. Zhidk. Gaza, No. 2 (1966).
24. S. J. Fenster, "Stagnation point heat transfer for a new binary air model, accounting for dissociation and ionization," Raketn. Tekh. Kosmon., 3, 12 (1965).
25. V. S. Avduevskii et al., Basic Theory of Space Vehicle Flight [in Russian], Mashinostroenie, Moscow (1972).
26. N. N. Yanenko, The Fractional Step Method for Solving Multidimensional Problems of Mathematical Physics [in Russian], Nauka, Novosibirsk (1967).
27. A. M. Grishin and V. N. Bertsun, "An iterative—interpolative method and the theory of splines," Dokl. Akad. Nauk SSSR, 214, 4 (1974).
28. J. H. Lundell and R. R. Dickey, "Graphite ablation at high temperatures," AIAA Paper 71-418 (1971).
29. T. A. Dolton, R. E. Maurer, and H. E. Goldstein, "Thermodynamic performance of carbon in hyperthermal environments," AIAA Paper 68-754 (1968).
30. V. N. Baranov, "Approximate analytical solution of the equations of motion during atmospheric entry," Kosm. Issled., 16, No. 3 (1978).